THE JOURNAL OF PHYSICAL CHEMISTRY A

Article

DFT Comparison of Fe Hydration in the Binding Sites of the Ferroxidase Center of Bullfrog M Ferritin

Daniel E. Bacelo, and R. C. Binning Jr.

J. Phys. Chem. A, **2009**, 113 (7), 1189-1198• Publication Date (Web): 26 January 2009

ARTICLES

DFT Comparison of Fe^{2+} Hydration in the Binding Sites of the Ferroxidase Center of Bullfrog M Ferritin

Daniel E. Bacelo* and R. C. Binning, Jr.

Department of Sciences and Technology, Universidad Metropolitana, P.O. Box 21150, San Juan, Puerto Rico 00928-1150

Received: August 11, 2008

Density functional theory optimizations have been conducted on structures of complexes of Fe^{2+} with $(H_2O)_n$ ($n = 0-3$) in three-residue models of binding sites A and B of the ferroxidase center of bullfrog M ferritin. Each site is modeled by the full structures of its three active amino acids. The potential surface at each site in the presence of water molecules is complex; coordination numbers of iron from three to six are seen. Water contributes to the complexity through its ability to hydrogen bond, to coordinate to iron, and to displace the neutral ligands glutamine and histidine. Intrinsic differences are noted at each site; at site B, the most stable complexes are found to favor tetracoordinate iron, while pentacoordination is preferred at site A in the two- and three-water complexes. While each incremental addition of a water molecule results in increased stability, successive binding energies are found to decrease.

Introduction

Ferritins are the principal iron storage proteins in animals, plants, and bacteria.[1,2] Animal ferritins consist of 24 subunits of two types, H and L, arranged as a hollow sphere. Each H subunit possesses a ferroxidase center. The mechanism of the ferroxidase reaction is incompletely understood, but the reaction proceeds from the binding of Fe^{2+} at sites A and B within the center, then to oxidation by O_2 to form a diiron(III) peroxodiferric intermediate that has been spectroscopically observed.[3] Decay of the intermediate to an oxide hydrate ensues, and the product is transported to the central cavity of the protein. The ferroxidase reaction is not the only path to iron(III) oxide, but it appears to initiate and accelerate the process.[4,5]

The amino acids crucial to the function of the center in bullfrog M (a variant of H) ferritin (FrMF) have been identified by a combination of crystallography, kinetics, and site-directed mutagenesis,[6] and the FrMF ferroxidase center is the subject of the present study. Site A of FrMF binds iron with two glutamates and a histidine, Glu23, Glu58, and His61. A glutamate, a glutamine, and an aspartate, Glu103, Gln137, and Asp140, comprise site B. Glu23 and Glu103 lie approximately along the site A−site B axis. The Glu, Glu−X−X−His motif of site A is conserved in all known vertebrate H ferritins, whereas considerable variation is found in the position 140 residue of site B. In bullfrog H, chicken M, and salmon H ferritin, the position is occupied by a serine, and in human H, bovine H, and salmon M ferritin by alanine.[6−8]

The ferroxidase center is a hydrophilic environment lying near the outer surface of its subunit, a surface that adjoins a hydrophilic channel along which Fe^{2+} is probably transported. Knowledge of hydration of bound Fe^{2+} is therefore likely to be crucial to understanding the energetics and mechanism of the initial phase of the ferroxidase reaction. Crystallography is the principal source of structural information on ferritin. Cocrystallization of cations with the apoprotein locates the ferroxidase sites. However, in the extant crystal structures, both sites are occupied, and there is little direct information on the binding of single ions, although kinetics studies do indicate that binding of Fe^{2+} is sequential.[9,10] Furthermore, little is known about water

TABLE 1: FrMf Site A−Fe^{2+} Water Cluster Energies[a]

waters	Figure	E_t (au)	ΔE (kcal/mol)	E_{nucrep} (au)
$(H_2O)_0$	1a	−2689.49079	0.0	3649.0
	1b	−2689.48581	3.1	3587.7
	1c	−2689.48452	3.9	3617.3
[b]$(H_2O)_1$	3a	−2765.98160	0.0	3848.4
	3b	−2765.97900	1.6	3871.1
	3c	−2765.97580	3.6	3884.6
	3d	−2765.96866	8.1	3894.9
	3e	−2765.96399	11.1	3796.5
$(H_2O)_2$	5a	−2842.46033	0.0	4117.5
	5b	−2842.45840	1.2	4006.4
	5c	−2842.45371	4.2	4118.6
	5d	−2842.45207	5.2	4079.2
	5e	−2842.44612	8.9	4151.8
	5f	−2842.44338	10.6	4158.6
	5g	−2842.44290	10.9	4161.7
$(H_2O)_3$	7a	−2918.93159	0.0	4395.1
	7b	−2918.92857	1.9	4438.0
	7c	−2918.92783	2.4	4358.2
	7d	−2918.92648	3.2	4300.4
	7e	−2918.92608	3.5	4374.7
	7f	−2918.92222	5.9	4378.5
	7g	−2918.91901	7.9	4448.9
	7h	−2918.90950	13.9	4392.2

[a] E_t is the total energy, ΔE is the energy relative to the global minimum, and E_{nucrep} is the nuclear repulsion energy. [b] $E_{H2O} = -76.46033$ au.

* Corresponding author. Fax: (787) 759-7663. E-mail: dbacelo@yahoo.com.

10.1021/jp807170b CCC: $40.75
Published on Web 01/26/2009

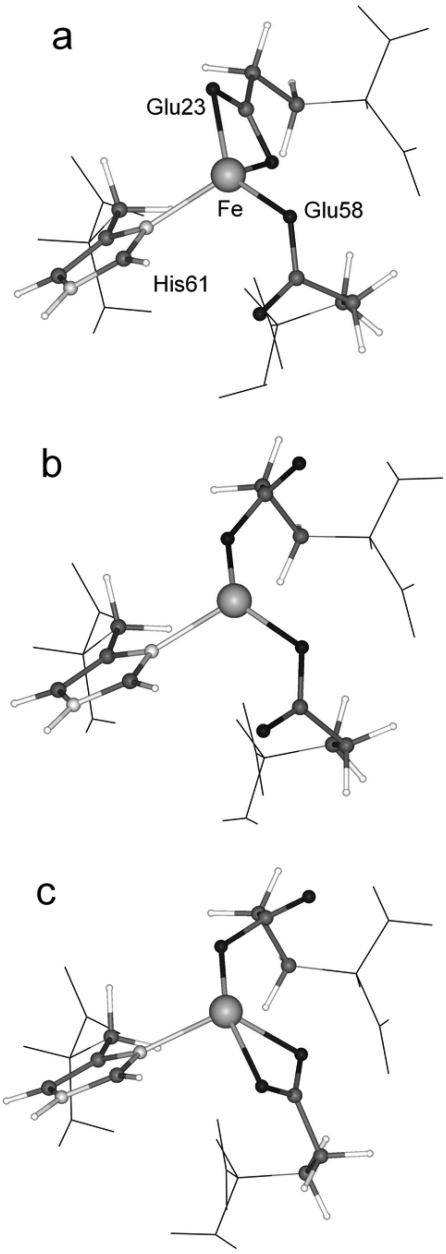

Figure 1. Optimized structures of Fe^{2+}−site A complexes. Oxygen atoms are black; carbons are dark gray; nitrogens and iron are light gray. Fixed backbone atoms are displayed as lines.

TABLE 2: FrMf Site B−Fe^{2+} Water Cluster Energies

waters	Figure	energy (au)	ΔE (kcal/mol)	E_{nucrep} (au)
$(H_2O)_0$	2a	−2633.16049	0.0	3235.1
	2b	−2633.14277	11.1	3271.9
$(H_2O)_1$	4a	−2709.64848	0.0	3452.8
	4b	−2709.64137	4.5	3397.5
	4c	−2709.63766	6.8	3504.6
	4d	−2709.63437	8.9	3357.6
	4e	−2709.61667	20.0	3523.8
$(H_2O)_2$	6a	−2786.12669	0.0	3689.5
	6b	−2786.11901	4.8	3644.0
	6c	−2786.11800	5.5	3705.7
	6d	−2786.11778	5.6	3600.7
	6e	−2786.11712	6.0	3658.6
	6f	−2786.11198	9.2	3742.2
	6g	−2786.10907	11.1	3760.2
$(H_2O)_3$	8a	−2862.60705	0.0	3904.3
	8b	−2862.59970	4.6	3964.3
	8c	−2862.59736	6.1	3958.0
	8d	−2862.59226	9.3	3989.7
	8e	−2862.58838	11.7	4000.9
	8f	−2862.58289	15.2	4024.8
	8g	−2862.58277	15.2	4023.8
	8h	−2862.57601	19.5	4054.5

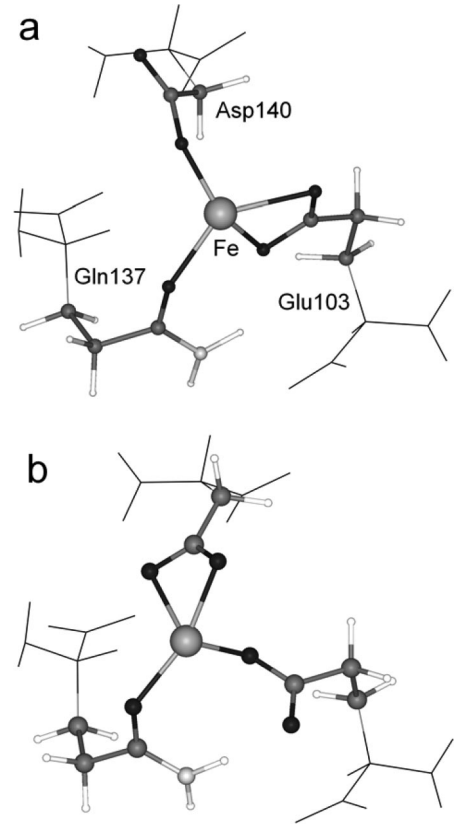

Figure 2. Optimized structures of Fe^{2+}−site B complexes.

molecules in the ferroxidase center, although water molecules have been observed.[4,11]

Theoretical modeling offers a means to supplement the limited information about water structure within the ferroxidase center. We have therefore conducted a study of the primary hydration sphere of Fe^{2+} bound at the two sites within the center, employing density functional electronic structure theory. Structures of complexes of Fe^{2+} at sites A and B with as many as three molecules of water, sufficient to saturate the primary coordination sphere of iron, have been optimized. A previous study of a sequence of complexes in the ferroxidase center of HuHF[12] showed that a simple model consisting of the six active amino acids provides structures consistent with the available experimental information. We here examine hydration at sites A and B, employing a similar three-residue model for each site.

To focus on the intrinsic properties of each site, calculations have been conducted on the two sites in isolation. The present study represents therefore a zeroth-order approach to the problem of hydration in the ferroxidase center in which interaction between them is ignored. The two sites are separated by about 5 Å, and there is interaction, especially when doubly occupied. In that light, the present work may be regarded as the initial step in defining the nature and magnitude of intersite interaction.

Methods

Geometries were optimized in spin-unrestricted density functional theory calculations with Fe^{2+} in its high-spin state. The BPW91 functional was employed. BPW91 consists of Becke's 1988 exchange functional[13] and the gradient-corrected correlation functional of Perdew and Wang.[14] Numerical basis sets of double numerical plus polarization quality (DNP) were employed. Optimizations were carried out with the Dmol[3]

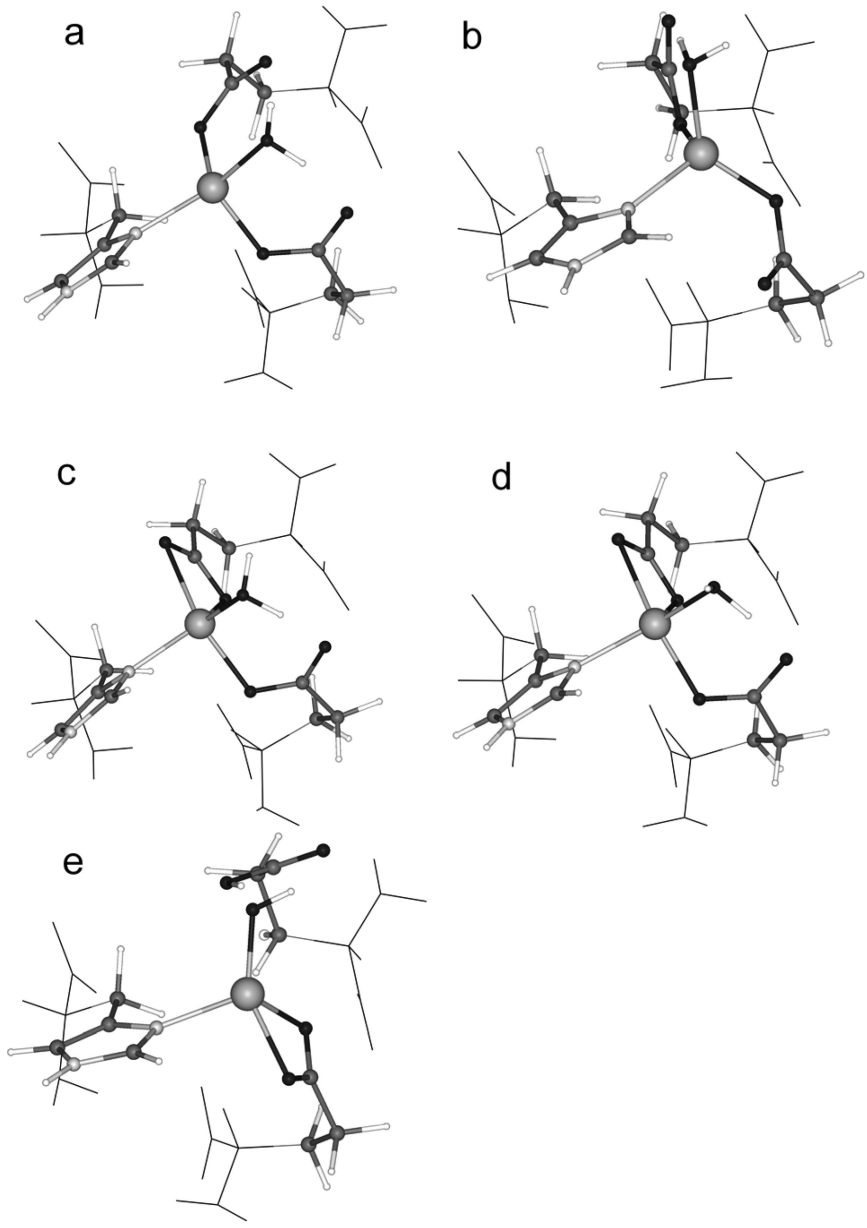

Figure 3. Optimized structures of Fe^{2+}−site A complexes with one water molecule.

program.[15,16] During optimization, four atoms in each amino acid, two carbons, a nitrogen, and an oxygen, comprising the amide-bonded backbone of the protein were fixed in their crystallographically determined[17] positions. Dangling bonds were capped with hydrogen atoms, and these were allowed to float during optimization.

Results and Discussion

Energies of the amino acid−iron−water complexes at sites A and B are presented, respectively, in Tables 1 and 2, accompanied by their designations in Figures 1−8. The site A optimized structures are presented in odd-numbered Figures 1−7, in respective order from zero- to three-water complexes, and displayed within each figure in ascending order in energy. Site B complexes, similarly organized, are shown in even-numbered Figures 2−8. Fe−ligand distances for the site A and B complexes are shown, respectively, in Tables 3 and 4. The presentation has been simplified by displaying only one example of the several energetically nearly degenerate rotational isomers found for some complexes. Complexes that present the opportunity for rotation about single bonds or hydrogen bonds can give rise to multiple molecular geometries that differ little in bonding and energy. Each set of clusters containing from zero to three water molecules is discussed in turn below.

Zero-Water Clusters. In the zero-water clusters, the interaction of Fe^{2+} with the amino acids in the absence of water molecules may be seen, and these form a basis from which to gauge changes that occur as the number of ligands increases. Indeed, some structural elements of the zero-water clusters will be found to persist throughout the study. Both the site A and the site B complexes follow the general rule that aspartate and glutamate bidentition in metalloproteins is most favored in complexes in which the central metal has unsaturated coordination.[18]

Despite the very different structures seen in the complexes at sites A and B, the optimized position of Fe^{2+} is fairly constant, varying by no more than 0.6 Å among all complexes. While the dominant interaction is electrostatic, some charge transfer is evident from population analysis. In structure 1a, for example, the Glu58 oxygen atom bonded to iron shows 0.12 electron spins

TABLE 3: FrMf Site A−Fe^{2+} Water Cluster Fe^{2+}−Ligand Distances (Å)

number of waters	Figure	ligand					
		O_{Glu23}	O_{Glu58}	N_{His61}	H_2O	H_2O	H_2O
zero	1a	2.118, 2.100	1.892	2.092			
	1b	1.866	1.881	2.098			
	1c	1.881	2.144, 2.114	2.133			
one	3a	1.965	1.975	2.118	2.074		
	3b	1.992	1.927	2.094	2.092		
	3c	2.030, 2.361	2.070	2.105	2.083		
	3d	2.035, 2.346	2.057	2.140	2.093		
	3e		2.153, 2.102	2.135	1.873[a]		
two	5a	2.088	1.986	2.159	2.071	2.344	
	5b	1.991	1.960		2.084	2.059	
	5c	2.005	1.934	2.095	2.068		
	5d	1.970	1.967	2.109	2.077		
	5e	2.034, 2.406	2.077	2.106	2.094		
	5f	2.040	1.952	2.190	2.123	2.402	
	5g	2.038, 2.313	2.134	2.134	2.097		
three	7a	2.039	2.060	2.159	2.100	2.358	
	7b	2.121	2.026	2.222	2.215	2.239	2.404
	7c	2.066	1.999	2.165	2.131	2.205	
	7d	2.007	2.015		2.116	2.390	2.115
	7e	1.992	2.073	2.192	2.232	2.152	
	7f	2.045		2.230	1.990[a]	2.151	2.317
	7g	2.043	1.982	2.225	2.149	2.286	
	7h	2.161, 2.139	2.076	2.160	2.160		

[a] The ligand is OH^-.

TABLE 4: FrMf Site B−Fe^{2+} Water Cluster Fe^{2+}−Ligand Distances (Å)

number of waters	Figure	ligand					
		O_{Glu103}	O_{Gln137}	O_{Asp140}	H_2O	H_2O	H_2O
zero	2a	2.080, 2.225	2.058	1.878			
	2b	1.976	1.978	2.044, 2.160			
one	4a	2.021	2.063	1.896	2.116		
	4b	2.228, 2.053		1.877	2.094		
	4c	2.095, 2.354	2.082	1.973	2.152		
	4d	1.971		1.854	2.039		
	4e	1.874	2.063	1.916	2.241		
two	6a	2.013	2.058	1.939	2.073		
	6b	2.269, 2.079		1.920	2.098	2.326	
	6c	2.064	2.158	1.904	2.307	2.226	
	6d	1.964		1.896	2.093	2.220	
	6e	2.020	2.060	1.907	2.103		
	6f	2.064	2.187	1.895	2.387	2.185	
	6g	2.036	2.058	1.893	2.102		
three	8a	2.031	2.069	1.935	2.037		
	8b	2.063	2.105	1.995	2.099	2.255	
	8c	2.048	2.133	1.928	2.108		
	8d	2.150	2.124	1.995	2.073	2.273	
	8e	2.119	2.214	1.961	2.339	2.224	2.380
	8f	2.111, 2.365	2.127	1.902	2.132		
	8g	2.111	2.166	2.026	2.384	2.155	2.358
	8h	2.378, 2.104	2.125	1.912	2.167		

of unpaired density and a slightly enhanced negative gross charge as compared to its companion oxygen that is not bonded. Population analysis places 6.4 electrons in the 3d subshell of Fe^{2+}, and this figure does not vary markedly from structure to structure nor show much dependence on coordination number.

Site A. Three complexes were optimized (Figure 1). They are structurally distinct but differ in energy by less than 4 kcal/mol. In the low-energy structure, 1a, iron is coordinated to four atoms, and Glu23 is bidentate. The Glu23 O−C−O bond angle is 119.0°, versus 123.3° in singly attached Glu58, and the $Fe-O_{Glu23}$ bond lengths, 2.10 and 2.12 Å, compare to 1.89 Å in $Fe-O_{Glu58}$ (Table 3). The least stable complex, 1c, is similar to 1a, except that in it Glu58 is bidentate. Thus, double attachment to iron by Glu23 is energetically favored over double attachment by Glu58. This result is consistent with crystallographic images of the dication complexes that show Glu23 both singly attached[4] to iron and doubly attached,[17] but Glu58 is never doubly attached; it is always seen bridging the two cations.

In the second most stable complex, 1b, neither glutamate is bidentate. Fe^{2+} is tricoordinate, with single attachments to a His61 nitrogen atom and oxygens of Glu23 and Glu58. The Fe−N distance of 2.10 Å is typical for $Fe^{2+}-N_{imidazole}$,[19] and the Fe−O distances, 1.87 and 1.88 Å, are also typical of carboxylate oxygen−iron(II) distances.[20] The nuclear repulsion energy (Table 1) of this complex is the lowest of the three, a source of stabilization that nearly offsets the fact that there are only three metal−ligand bonds.

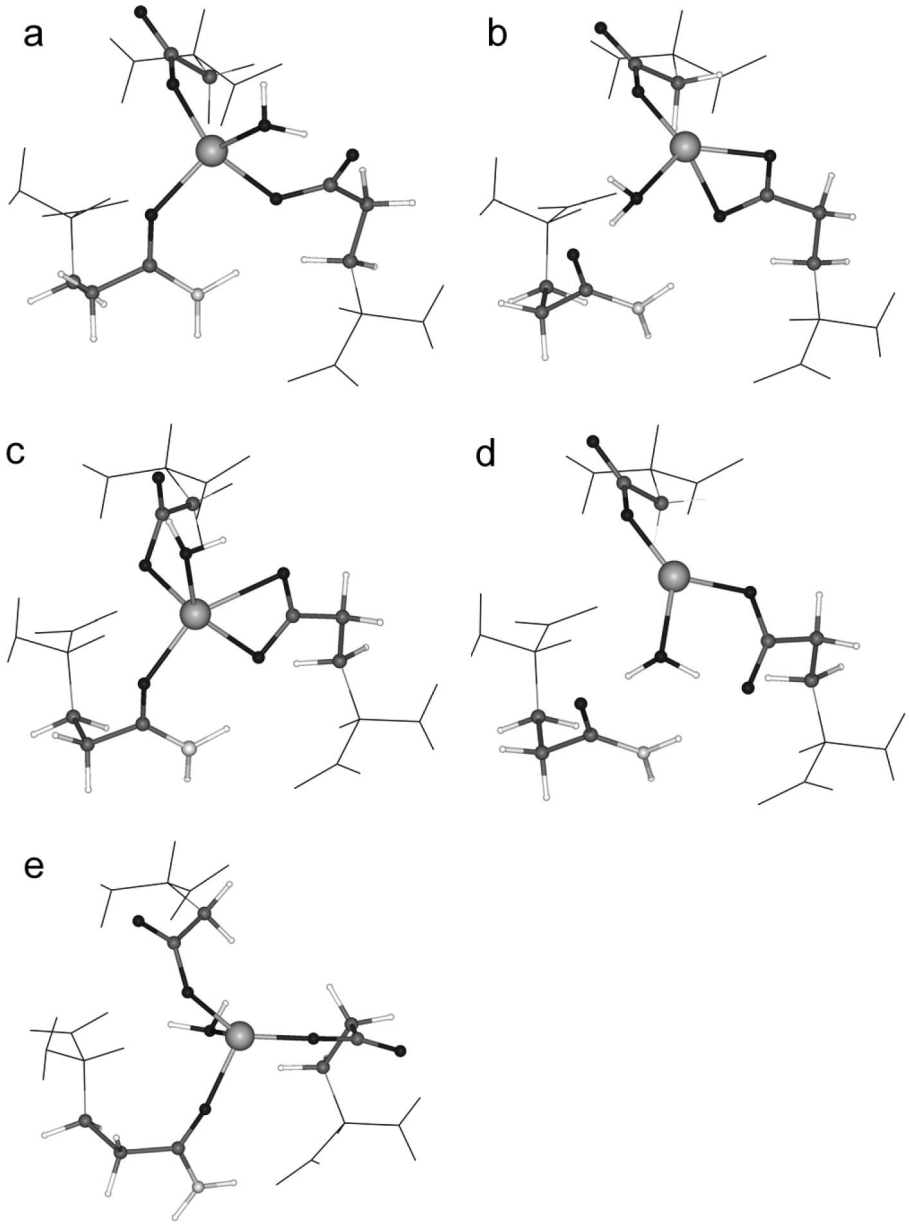

Figure 4. Optimized structures of Fe^{2+}−site B complexes with one water molecule.

Site B. In contrast to the case with the site A isomers, the two site B complexes shown in Figure 2 are well separated in energy. In complex 2a Glu103 is bidentate, and there are single attachments to oxygen atoms of Gln137 and Asp140. In addition, Gln137−NH_2 hydrogen bonds to one of the attached oxygens of Glu103. This Gln137−Glu103 hydrogen bond recurs in the majority of the site B structures.

Structure 2b has a bidentate Asp140, and it lies 11.1 kcal/mol in energy higher than 2a. Detaching one of the oxygens of Glu103 has some stabilizing effects. A stronger hydrogen bond to −NH_2 of Gln137 (shorter by almost 0.2 Å) can be formed by that oxygen atom, and the Fe−O bond to Gln137 is shorter than that in structure 2a, yet the complex is much less stable. The situation seems to be confirmed crystallographically,[17] where Asp140 is singly attached to Mg^{2+}. Glu103 appears to be bidentate in HuHF[4] and *E. coli* nonheme ferritin,[21] but in FrMF one oxygen seems to be directed toward the hydroxyl group of a tyrosine. The distance between the two, however, suggests that an associated water molecule is present.

One-Water Clusters. Adding a molecule of water to either site A or B results in markedly more stable complexes. The energy difference between the average zero- and one-water site A complexes (see Table 1) is 16.6 kcal/mol, and the corresponding difference for site B complexes (Table 2) is 14.9 kcal/mol. The added water provides an additional ligand for the iron ion, and it can also stabilize a dangling carboxylate oxygen with a hydrogen bond. In the site B complexes, water is seen to effectively displace glutamine from the coordination sphere of iron. In both sites A and B, the low-energy forms feature a tetracoordinate iron with no bidentate ligands.

Site A. Five isomers are displayed in Figure 3. The two low-energy isomers are similar. They feature tetracoordination about iron, with singly attached glutamates, and differ only in the hydrogen bonding of the water molecule. Water in the global minimum energy structure, 3a, hydrogen bonds to oxygens of both Glu23 and Glu58. In 3b, there is a single hydrogen bond to Glu23.

In structures 3c and 3d, the hydrogen bond is to Glu58, while both carboxylate oxygens of Glu23 are attached to iron. The double attachment is asymmetric, with Fe−O distances of 2.03 and 2.35 Å. The two apparently differ only by a rotation about the hydrogen bond, but they are both included in Figure 3

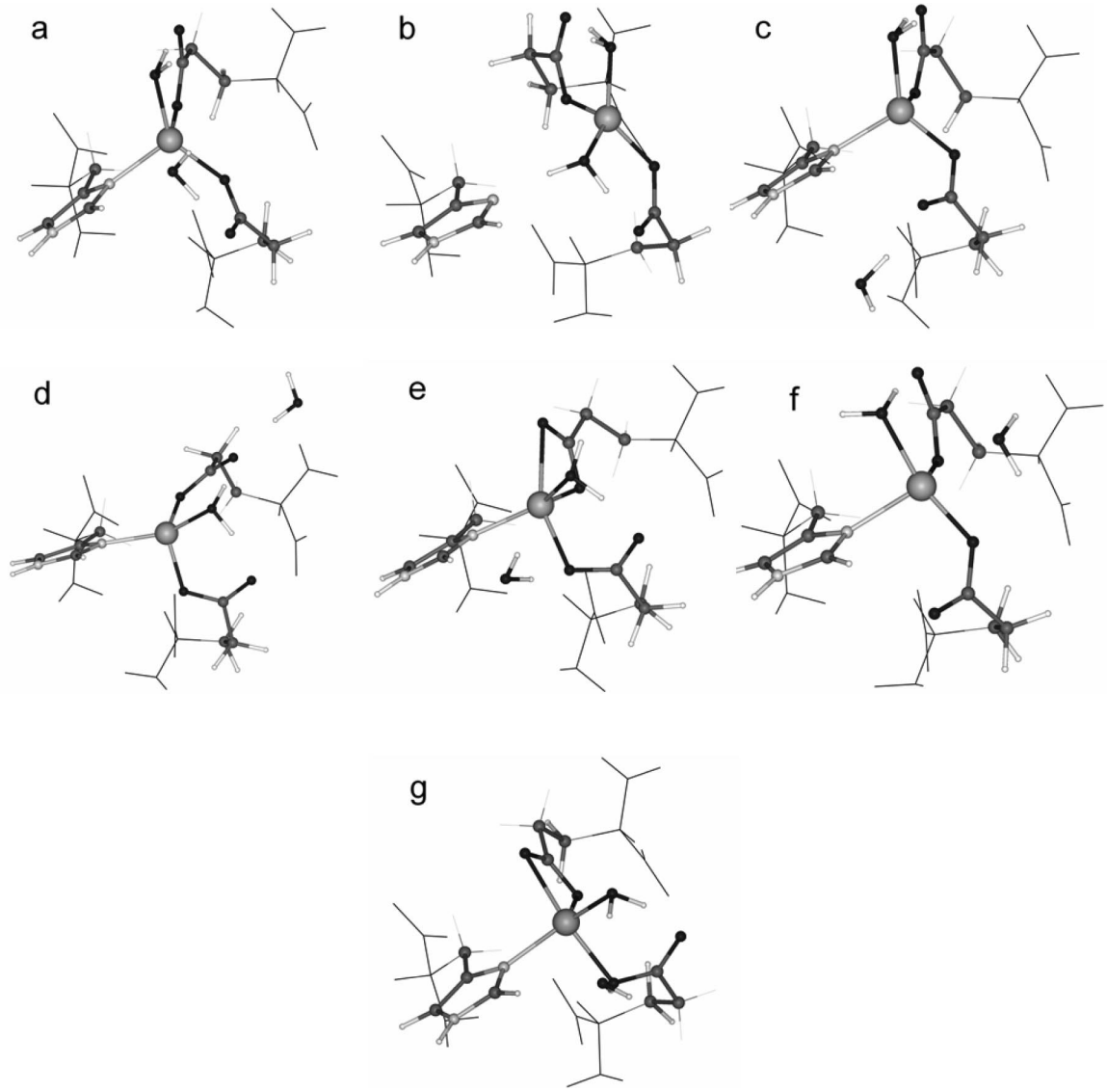

Figure 5. Optimized structures of Fe^{2+}−site A complexes with two molecules of water.

because they differ in energy by more than 4 kcal/mol. The origin of the difference is not obvious, but 3c is significantly lower in nuclear repulsion energy, indicating that steric effects in 3d are responsible.

The isomer highest in energy (Figure 3e) lies 11.1 kcal/mol above the global minimum. It is interesting in that it features a dissociated water molecule and a protonated glutamate, but its relatively high energy shows that dissociation of water in complexes with iron(II) is unfavorable.

Site B. The five one-water site B clusters (Figure 4) display a wider range of energies than do their site A counterparts, and the structures are well-separated in energy. Complexes 4b−4e lie 4.5, 6.8, 8.9, and 20.0 kcal/mol, respectively, above the global minimum energy (Table 2). Three structures feature tetracoordinate iron, and one each tri- and pentacoordination.

As in site A, the two lowest energy clusters exhibit a tetracoordinate iron. They are distorted from tetrahedral, with single attachments from oxygens of the water molecule, Glu103, Gln137, and Asp140 in the case of the global minimum, 4a. In complex 4b, Gln137 has been displaced by water, whereas Glu103 is doubly attached. Gln137 is bound by hydrogen bonds to both ends of its formamidyl group. Pentacoordinate complex 4c with bidentate Glu103 and tricoordinate 4d, in which Gln137 is again not directly attached to iron, are close in energy. Stabilizing factors for complex 4d are the facts that its nuclear repulsion energy is lowest in its group, and that its water molecule, besides being attached to iron, forms two hydrogen bonds.

The high-energy complex, 4e, is one in which H_2O is hydrogen bonded to an oxygen atom that forms part of the backbone of the protein. The proximity to the backbone results in this complex having the highest nuclear repulsion energy of the group, and it illustrates that the region away from the binding site itself is hydrophobic.

Two-Water Clusters. Two water molecules provide the freedom to form pentacoordinate structures about the metal with singly attached ligands. They also introduce an added element of structural complexity in their potential to hydrogen bond to each other. However, the stabilization due to addition of a molecule of water to the one-water complexes falls from that of addition to a zero-water complex. The average stabilization energies are 10.6 kcal/mol for the site A complexes and 13.2 kcal/mol for the site B.

Site A. The site A two-water clusters are depicted in Figure 5. In the global minimum-energy complex, 5a, iron is pentacoordinate. An oxygen from each glutamate, a nitrogen from

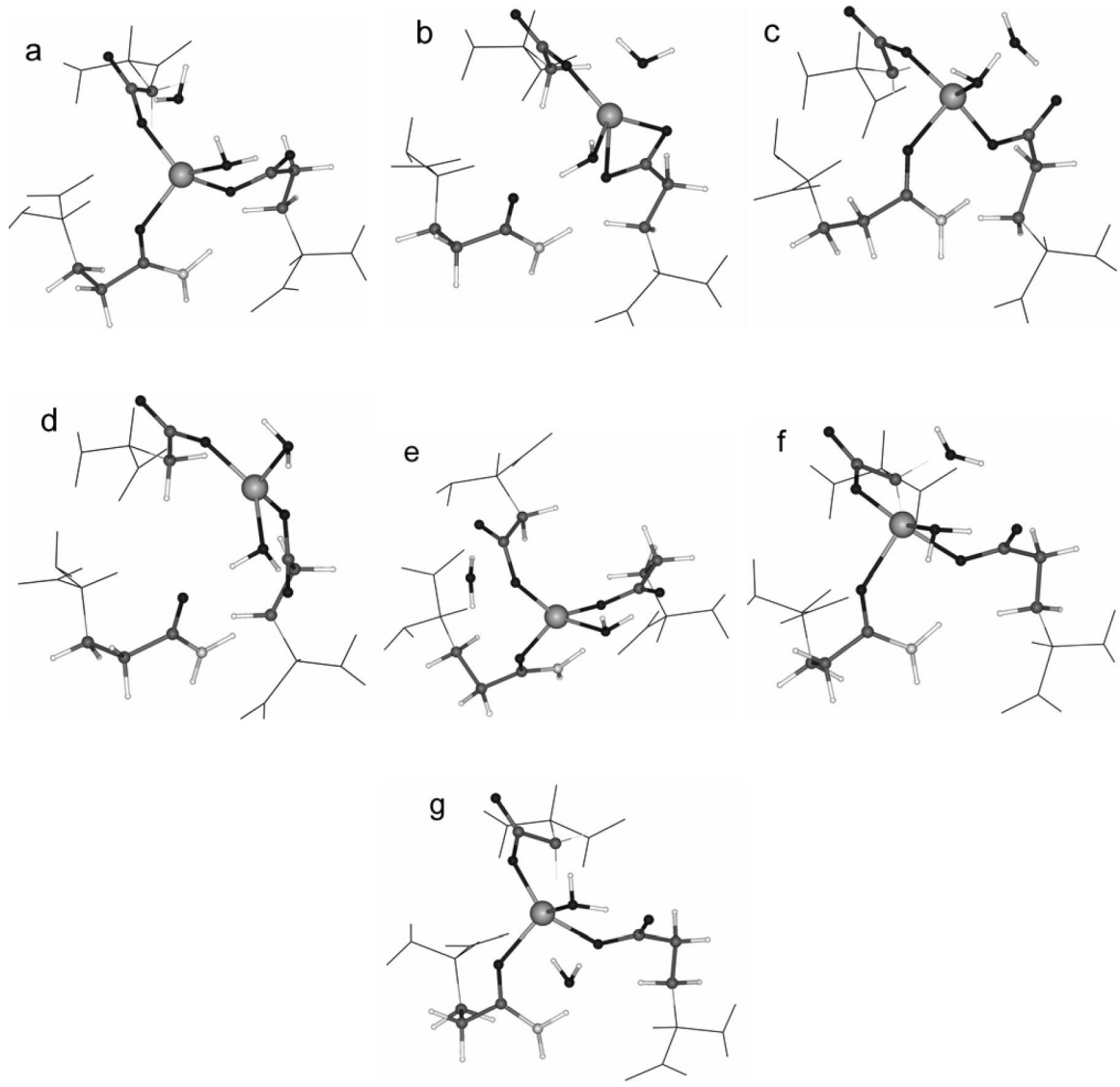

Figure 6. Optimized structures of Fe^{2+}−site B complexes with two molecules of water.

histidine, and two waters coordinate to iron, arranged roughly as a trigonal bipyramid. Each water molecule is hydrogen bonded to a free glutamate oxygen, forming two cyclic substructures within the complex. One water is tightly held to the metal (2.07 Å), while Fe−O in the second is 2.34 Å. Only 1 kcal/mol higher in energy than the global minimum is a tetracoordinate structure, roughly tetrahedral about iron, which differs from the low-energy structure primarily in that the imidazolyl group of histidine is not attached to iron; it is hydrogen-bonded to the water molecule that has displaced it. The reduced crowding around iron and the hydrogen bond nearly compensate for the loss of the Fe−N bond energy, although imidazole is a stronger ligand for Fe^{2+} than is water.[19]

Two similar tetracoordinate complexes lie 4−6 kcal/mol above the minimum, each having one water molecule that is not coordinated to iron but hydrogen bonded to the free oxygens of Glu23 and Glu58, respectively. Grouped at 9−11 kcal/mol above the minimum are three pentacoordinate structures, two of which, 5e and 5g, feature a bidentate Glu23 with a single water molecule attached to iron, while in the third (5f) both water molecules are attached to Fe^{2+}, although one of the attached waters participates in no hydrogen bonds and, although coordinated to Fe^{2+}, lies 2.41 Å from it (Table 3).

Site B. Seven clusters are displayed in Figure 6. Four feature tetracoordination about iron, and three are pentacoordinate. An example of bidentition is found in a pentacoordinate complex. The complexes group by energy into three segments. The low-energy complex, 6a, is well separated from the rest, 4.8 kcal/mol below the next lowest. It has one water molecule attached to iron, while the second is free, hydrogen bonded to the bound water and to the Asp140 carboxylate oxygen that is coordinated to Fe^{2+}.

Four complexes, 6b−6e, that lie within 1.2 kcal/mol of each other comprise the second tier. The two pentacoordinate complexes, 6b and 6c, have both water molecules attached to Fe^{2+}, although in each Fe−O is more than 2.3 Å (Table 4). In two, 6b and 6d, a water molecule displaces Glu137 from its attachment to Fe^{2+}, but in each both ends of the formamidyl participate in hydrogen bonds. Complex 6e has a water molecule that is attached only to the free oxygen atom of Asp140.

Finally, there are two high-energy complexes, 6f and 6g, lying 9.2 and 11.1 kcal/mol above the global minimum. In 6f, one water molecule is rather weakly coordinated to iron (2.4 Å) and also rather weakly hydrogen bonded to a carboxylate oxygen of Glu103 (O−H = 2.1 Å). Similarly, complex 6g has a weakly attached water molecule that has only one hydrogen bond, again

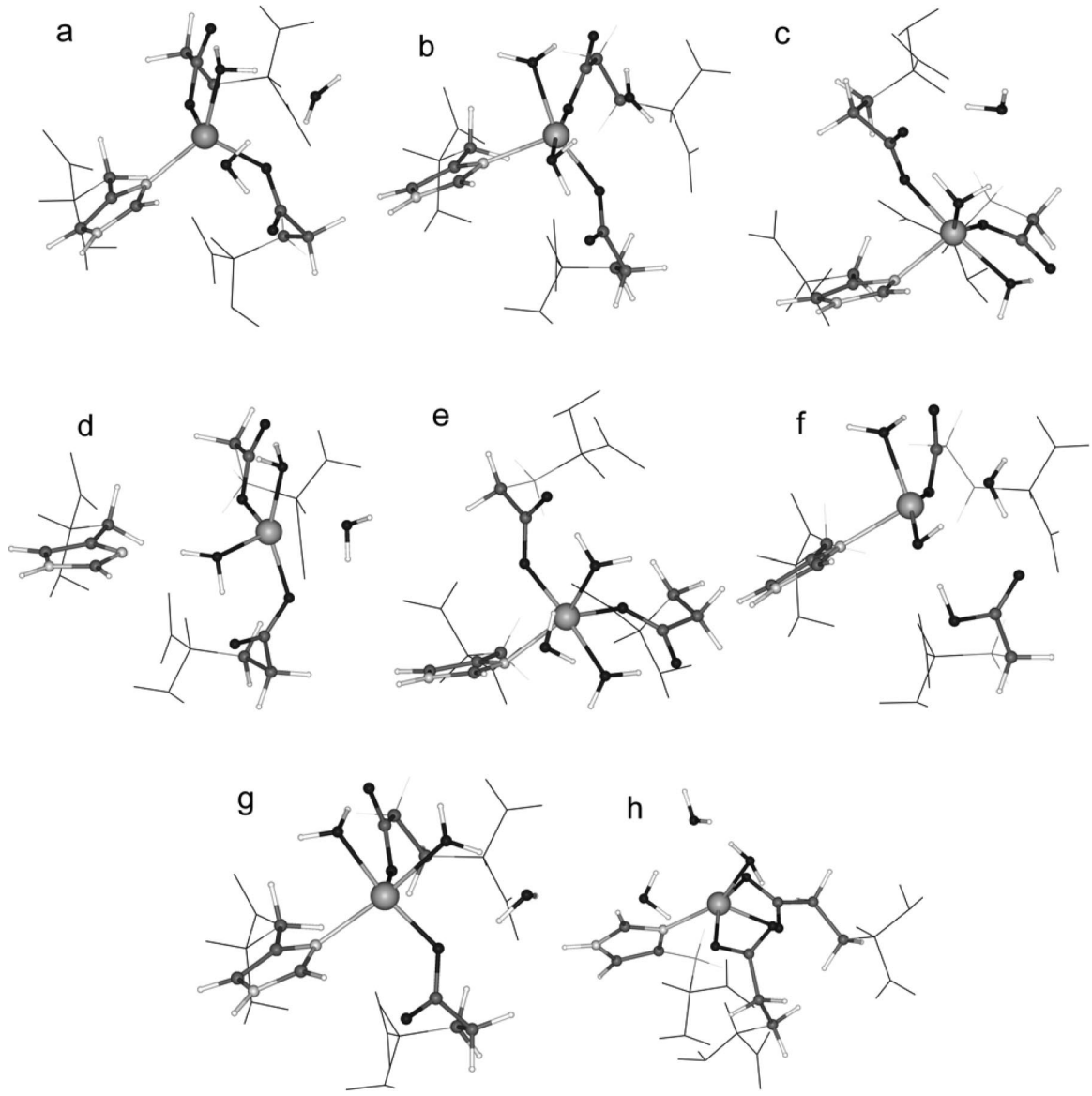

Figure 7. Optimized structures of Fe^{2+}−site A three-water complexes.

to a carboxylate oxygen of Glu103. Complexes 6f and 6g have the highest nuclear repulsion energies of the group, implicating steric effects in their relative instability.

Three-Water Clusters. With three water molecules iron can be coordinated by six singly attached ligands, but hexacoordination does not yield the most stable complexes in either site. With the three-water clusters, we can begin to examine the trends that accompany progressive hydration. Again, the addition of a molecule of water stabilizes the three-water complexes with respect to the two-water but by less than the corresponding addition stabilizes the two-water with respect to the one-water complexes. The stabilizing effect of adding water is thus seen to decline progressively (Tables 1 and 2). The average site A complex is 7.9 kcal/mol more stable than the average two-water complex plus a free water, and at site B the stabilization is 8.4 kcal/mol. An increase in the number of ligands has noticeable effects on geometries. For example, at site A as the number of water molecules increases from zero to three the average Fe−O distance to singly attached Glu23 increases from, respectively, 1.874 to 1.979 to 2.019 to 2.045 Å (Table 3). The average Gln137 Fe−O distances in site B complexes are 2.018, 2.069, 2.104, and 2.133 Å, respectively, for the 0−3 water clusters (Table 4).

Crowding is important in the three-water site B complexes, as evidenced by the fact that the energy ordering of total energies, with two minor exceptions, follows the ordering of the nuclear repulsion energies. At site A, the average nuclear repulsion energies in the complexes of from 0−3 water molecules are, respectively, 3618.0, 3859.1, 4113.4, and 4385.8 hartree. The incremental increases are 232.0, 236.1, and 245.1 hartree, respectively, excluding the intramolecular repulsion energy of water in its optimized geometry, 9.1 hartree, from each successive increment. The rate of increase is steeper at site B where respective average repulsion energies are 3253.5, 3447.3, 3685.8, and 3990.0 hartree, and incremental increases are 184.7, 220.3, and 276.9 hartree.

Site A. Figure 7 displays eight three-water complexes, seven of which have pentacoordinate iron and one hexacoordinate. Factors already noted in the discussion of two-water clusters govern the relative stability among the three-water clusters. Principal among these are the formation of interwater hydrogen bond structures as well as hydrogen bonds to unattached glutamate oxygen atoms.

In the global minimum energy structure, 7a, two water molecules are attached directly to Fe^{2+}; one is hydrogen bonded both to a glutamate oxygen and to another water

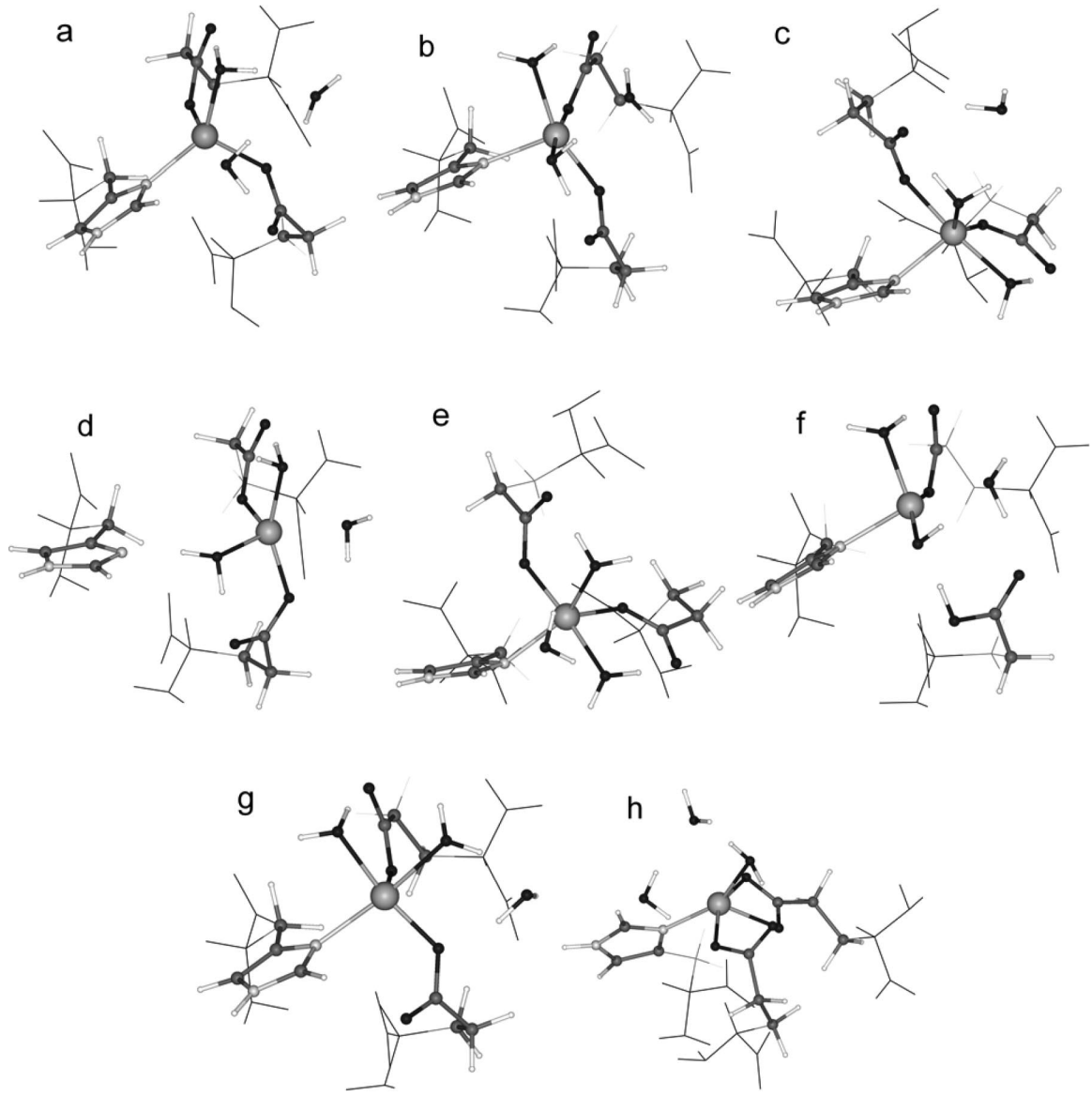

Figure 8. Optimized structures of Fe^{2+}−site B three-water complexes.

molecule. The double hydrogen bonds seem to pull the water somewhat away from Fe^{2+}; the Fe−O distance is 2.36 Å as compared to 2.10 Å for its companion, although both water molecules participate in two hydrogen bonds. Spacing approaches trigonal bipyramidal; the largest deviation of an equatorial ligand−Fe−ligand angle from 120° is the 133.2° of the imidazolyl−N−Fe−OH_2. The angle of the axial H_2O−Fe−O_{Glu23} is 173.8°. An additional stabilizing factor for the complex is the trigonal hydrogen bonded substructure among the three water molecules.

Although only one hexacoordinate complex (Figure 7b) was optimized, it is nearly as stable as the global minimum energy complex. The Fe−O distance to the additional water is rather long (2.40 Å). All three water molecules are attached to iron and participate in hydrogen bonds with free glutamate oxygens to form cyclic substructures. Two waters hydrogen bond to the same Glu23 oxygen atom to form a bicyclic structure.

Above this, but all within 4 kcal/mol of the global minimum, are three more pentacoordinate structures, 7c−7e. The structure of 7c is similar to that of 7a, but with a water molecule attached only by a hydrogen bond to Glu23. A loosely attached water is also the most notable feature of 7e; in this case, it is a double hydrogen-bond donor to the remaining waters. In 7d all three waters are attached to iron, although one is 2.4 Å distant, and His61 is displaced. Although the structure is quite different from those of the other two in the group, it exhibits the lowest nuclear repulsion energy, and the energy differences among them are small.

The three high-energy isomers, 7f−7h, each exhibit specific destabilizing factors. Complex 7f features a dissociated water molecule; in 7g one of the carboxylate oxygens of Glu58 does not participate in a hydrogen bond, and in 7h only one water molecule is coordinated to iron, while Glu58 is doubly attached.

Site B. There is considerable structural variation, with four-, five-, and six-coordination around iron (Figure 8). Three of the eight structures are low-lying; the rest are all more than 9 kcal/mol above the global minimum. The two common factors in the stability of the two low-energy isomers are that the carboxylate oxygens of Asp140 and Glu103 that are not coordinated toward iron are occupied with hydrogen bonds and that each water molecule participates in two hydrogen bonds. The third of the low-energy three, 8c, shares the latter trait, but

its Asp140 has a dangling oxygen atom. The global minimum energy structure, 8a, is tetracoordinate, and its very low nuclear repulsion energy must be cited as the major contributor to its relative stability.

The relative instabilities of the remaining five complexes are attributable to a variety of factors. In 8d both free carboxylate oxygens are occupied in hydrogen bonds, but one water can form only one hydrogen bond and another only a weak one (2.05 Å) to an Asp140 oxygen atom. In the two hexacoordinate complexes, 8e and 8g, all three waters are attached to iron, but two of these are rather weakly attached (Fe−O = 2.33 and 2.36 Å), and none are positioned to form more than one hydrogen bond. The structures of Figure 8f and h feature a bidentate Glu103 and floating water molecules that are bound only by a single hydrogen bond.

Conclusions

The potential energy surfaces of sites A and B hydrated iron(II)−FrMF ferroxidase are complex, rendered so by a number of competing factors. Among these are strong iron−carboxylate bonding, which may be either mono- or bidentate, the weaker iron−neutral ligand bonding, hydrogen bonding, and steric effects. The versatility with which water molecules bond facilitates formation of structurally diverse but energetically similar complexes. Waters compete for positions in the coordination sphere with the neutral ligands, histidine, and glutamine. The loss of metal−ligand bond energy in such displacements is compensated by Fe−water interaction energy, hydrogen bonds, and lowered internuclear repulsion. The variety of structures is consistent with the function of the ferroxidase center as one where a diiron oxide substrate is constructed and probably proceeds through several intermediates before being released. The presence of water molecules in the ferroxidase center is energetically favored, and it is therefore plausible that as many as three molecules of water per site are present during the initial phase of the ferroxidase reaction.

Crowding is important, more so at site B than at site A. In each set of site B complexes, the most stable complex features tetracoordinate iron. At site A, the most stable zero- and one-water complexes are tetracoordinate, but in the two- and three-water complexes the metal is pentacoordinate, and in the three-water case a hexacoordinate complex lies very low in energy. In the site B three-water complexes, the ordering of total energies (Table 2) nearly follows that of the nuclear repulsion energies.

The incremental increases in nuclear repulsion energy as water molecules are added to site B increase at a faster rate than do those of site A, indicating that space in the site is at a premium. This observation bears on the fact that the energies of the site B complexes are well separated, while site A has complexes more closely spaced in energy and more that are low-energy. At both sites the number of low-energy isomers, those lying within about 5 kcal/mol of the global minimum, does not increase rapidly. At site A there are three low-lying zero-water isomers ranging up to five three-water isomers. At site B there is one low-energy zero-water isomer and two low-energy three-water isomers.

The site B complexes are separated more in energy, on average, than are their site A counterparts. The average energy difference between the global minimum energy complex and the second lowest in energy is 2.0 kcal/mol at site A, 4.6 kcal/mol at site B, even excluding the wide interval in the zero-water case. The average difference between the low-energy and high-energy isomers is 10.0 kcal/mol for site A, as compared to 15.6 kcal/mol for site B. Several trends are apparent. Comparable metal−ligand distances generally increase with increasing metal coordination number. Incremental addition of water molecules stabilizes the complexes, but the incremental stabilization diminishes. Whether stabilization with the addition of water molecules beyond the primary coordination sphere approaches an asymptote or rapidly disappears is an important question, and an exploration of the second hydration shell would therefore be of interest.

Acknowledgment. We gratefully acknowledge the support of this research by the National Science Foundation in the form of Grant No. MCB-0641269.

References and Notes

(1) Liu, X.; Theil, E. C. *Acc. Chem. Res.* **2005**, *38*, 167.
(2) Chasteen, N. D.; Harrison, P. M. *J. Struct. Biol.* **1999**, *126*, 182.
(3) Hwang, J.; Krebs, C.; Huynh, B. H.; Edmondson, D. E.; Theil, E. C.; Penner-Hahn, J. E. *Science* **2000**, *287*, 122.
(4) Toussaint, L.; Bertrand, L.; Hue, L.; Crichton, R. R.; Declercq, J. P. *J. Mol. Biol.* **2007**, *365*, 440.
(5) Zhao, G.; Su, M.; Chasteen, N. D. *J. Mol. Biol.* **2005**, *352*, 467.
(6) Liu, X.; Theil, E. C. *Proc. Natl. Acad. Sci. U.S.A.* **2004**, *101*, 8557.
(7) Hempstead, P. D.; Yewdall, S. J.; Fernie, A. R.; Lawson, D. M.; Artymiuk, P. J.; Rice, D. W.; Ford, G. C.; Harrison, P. M. The Protein Data Bank, 2FHA. *J. Mol. Biol.* **1997**, *268*, 424.
(8) Lawson, D. M.; Artymiuk, P. J.; Yewdall, S. J.; Smith, J. M. A.; Livingstone, J. C.; Treffry, A.; Luzzago, A.; Levi, S.; Arosio, P.; Cesareni, G.; Thomas, C. D.; Shaw, W. V.; Harrison, P. M. *Nature* **1991**, *349*, 541.
(9) Bou-Abdallah, F.; Zhao, G.; Mayne, H. R.; Arosio, P.; Chasteen, N. D. *J. Am. Chem. Soc.* **2005**, *127*, 3885.
(10) Treffry, A.; Zhao, Z.; Quail, M. A.; Guest, J. R.; Harrison, P. M. *Biochemistry* **1997**, *36*, 432.
(11) Swartz, L.; Kuchinskas, M.; Li, H.; Poulos, T. L.; Lanzilotta, W. N. *Biochemistry* **2006**, *45*, 4421.
(12) Bacelo, D. E.; Binning, R. C. *Inorg. Chem.* **2006**, *45*, 10263.
(13) Becke, A. D. *Phys. Rev. A* **1988**, *38*, 3098.
(14) Perdew, J. P.; Burke, K.; Wang, Y. *Phys. Rev. B* **1996**, *54*, 16533.
(15) Delley, B. *J. Chem. Phys.* **1990**, *92*, 508.
(16) Delley, B. *J. Chem. Phys.* **2000**, *113*, 7756.
(17) Ha, Y.; Shi, D.; Small, G. W.; Theil, E. C.; Allewell, N. M. *J. Biol. Inorg. Chem.* **1999**, *4*, 243.
(18) Dudev, T.; Lim, C. *Acc. Chem. Res.* **2007**, *40*, 85.
(19) Ricca, A.; Bauschlicher, C. W. *J. Phys. Chem. A* **2002**, *106*, 3219.
(20) Marino, T.; Toscano, M.; Russo, N.; Grand, A. *J. Phys. Chem. B* **2006**, *110*, 24666.
(21) Stillman, T. J.; Hempstead, P. D.; Artymiuk, P. J.; Andrews, S. C.; Hudson, A. J.; Treffry, A.; Guest, J. R.; Harrison, P. M. *J. Mol. Biol.* **2001**, *307*, 587.

JP807170B